Drift Tube Studies of Large Carbon Clusters: New Isomers and the Mechanism of Giant Fullerene Formation

Joanna M. Hunter[†] and Martin F. Jarrold*

Contribution from the Department of Chemistry, Northwestern University, 2145 Sheridan Road, Evanston, Illinois 60208

Received May 22, 1995[⊗]

Abstract: Injected ion drift tube techniques, including ion mobility measurements and annealing and fragmentation studies, have been used to examine even-numbered carbon cluster cations containing 100−320 atoms. The drift time distributions reveal the presence of several families of geometric isomers. The single-shell fullerene remains the dominant isomer for clusters containing up to 320 atoms. In addition, a small component of nested cage fullerenes may be present for the larger clusters. The polycyclic polyyne ring isomers, which are abundant for clusters with less than 70 atoms, vanish at around 160 atoms. There is no evidence for the presence of long polyacetylene chains. A new family of isomers, a broad distribution with mobilities smaller than the fullerene but larger than the polycyclic rings, appears at around 100 atoms and slowly increases in relative abundance with increasing cluster size. These new isomers are probably the coalescence products of fullerenes and rings. When collisionally excited, a small fraction of these isomers readily dissociate, primarily by loss of C_{18} and larger even-numbered fragments, while the remainder appear to anneal into the fullerene structure. The estimated activation energy for this process is similar to the activation energy for conversion of the smaller polycyclic ring isomers into fullerenes.

Introduction

Although abundant fullerenes such as C_{60} and C_{70} have been well characterized, in both the gas and condensed phases, not much is known about carbon clusters containing 100−1000 atoms. Recent electron microscope and scanning tunneling microscope studies of various types of carbon soot have revealed the presence of unusual nanostructures such as nested fullerenes[1] and a variety of nanotubes.[2,3] However, the nature of the structural evolution that occurs between fullerenes and these large carbon nanostructures remains unexplored. There is some evidence from gas-phase experiments for the existence of giant fullerenes. Carbon clusters containing up to several hundred atoms have been formed by pulsed laser vaporization and examined by mass spectrometry.[4,5] Carbon clusters (presumably fullerenes) with masses greater than 3000 amu have been observed in laser desorption mass spectrometry investigations of arc-generated soot extract.[6] In addition, scanning tunneling microscope images of the extract obtained by high-pressure and high-temperature bomb extraction of arc generated soot show roughly spherical structures, 1−2 nm in diameter, which may be fullerenes containing up to 330 atoms.[7] Transmission electron microscope images of much larger carbon clusters (containing several thousand atoms) suggest that these species can exist as nested fullerene cage structures, called bucky-onions.[1] Multishell fullerenes are expected to become more stable than single-shell fullerenes for large carbon clusters. There have been several attempts to predict where this crossover in stability occurs. The predicted location depends on the method of calculation, ranging from around 700 to 6000 atoms.[8,9] Recently, it has been suggested that important isomers for the larger carbon clusters have an entirely different type of geometry, long polyacetylene chains.[10] As will be described below, we find no evidence for the presence of these isomers.

In this article we report a study of carbon cluster cations with 100−320 atoms using injected ion drift tube techniques. We will describe the results of ion mobility measurements along with the results of annealing and fragmentation studies. Ion mobilities are measured by determining the amount of time it takes for the ions to travel across a drift tube under the influence of a weak electric field. These measurements provide information about structural isomers that are present because the mobility of a gas-phase ion depends on its average collision cross section, which in turn depends on the geometry. Thus structural isomers can be separated as they travel across the drift tube. However, the separation that occurs in a drift tube is not chromatography,[11] the ions are separated on the basis of their differing mobilities. Although first demonstrated close to 20 years ago,[12,13] this approach has only recently been applied to atomic clusters.[14]

Previous drift tube studies of carbon cluster ions containing up to 70 atoms have revealed the presence of fullerenes

[†] Present address: SRI International, Molecular Physics Laboratory, 333 Ravenswood Ave., Menlo Park, CA 94025.

[⊗] Abstract published in *Advance ACS Abstracts*, October 1, 1995.

(1) Ugarte, D. *Nature* **1992**, *359*, 707.
(2) Iijima, S. *Nature* **1991**, *347*, 354. Ebbesen, T. W.; Ajayan, P. M. *Nature* **1992**, *358*, 220.
(3) Ge, M.; Sattler, K. *Science* **1993**, *260*, 515.
(4) Rohlfing, E. A.; Cox, D. M.; Kaldor, A. *J. Chem. Phys.* **1984**, *81*, 3322. Cox, D. M.; Reichmann, K. C.; Kaldor, A. *J. Chem. Phys.* **1988**, *88*, 1588.
(5) McElvaney, S. W.; Nelson, H. H.; Baronavski, A. P.; Watson, C. H.; Eyler, J. R. *Chem. Phys. Lett.* **1987**, *134*, 214.
(6) Parker, D. H.; Chatterjee, K.; Wurz, P.; Lykke, K. R.; Pellin, M. J.; Stock, L. M. *Carbon* **1992**, *30*, 1167.
(7) Lamb, L. D.; Huffman, D. R.; Workman, R. K.; Howells, S.; Chen, T.; Sarid, D.; Ziolo, R. F. *Science* **1992**, *255*, 1413.
(8) Tománek, D.; Zhong, W.; Krastev, E. *Phys. Rev. B* **1993**, *48*, 15461.
(9) Maiti, A.; Brabec, C. J.; Bernholc, J. *Phys. Rev. Lett.* **1993**, *70*, 3023.
(10) Lagow, R. J.; Kampa, J. J.; Wei, H. C.; Battle, S. L.; Genge, D. A.; Laude, D. A.; Harper, C. J.; Bau, R.; Stevens, R. C.; Haw, J. F.; Munson, E. *Science* **1995**, *267*, 362.
(11) Spangler, G. E.; Carrico, J. P. *Int. J. Mass Spectrom. Ion Proc.* **1983**, *52*, 267.
(12) See, for example: Tou, J. C.; Boggs, G. U. *Anal. Chem.* **1976**, *48*, 1351. Carr, T. W. *J. Chromatogr.* **1977**, *15*, 85. Hagen, D. F. *Anal. Chem.* **1979**, *51*, 870. Karpas, Z.; Cohen, M. J.; Stimac, R. M.; Wernlund, R. F. *Int. J. Mass Spectrom. Ion Proc.* **1986**, *83*, 163.
(13) For a recent review see: St. Louis, R. H.; Hill, H. H. *Crit. Rev. Anal. Chem.* **1990**, *21*, 321.
(14) von Helden, G.; Hsu, M.-T.; Kemper, P. R.; Bowers, M. T. *J. Chem. Phys.* **1991**, *95*, 3835.

0002-7863/95/1517-10317$09.00/0

containing as few as 30 atoms and a variety of polyyne rings which have been attributed to monocylic, bicyclic, tricyclic, and tetracyclic rings.[15] An important feature of the injected ion drift tube technique is that it can be used to examine structural interconversions.[16] As the ions are injected into the drift tube they undergo collisions with the buffer gas which transiently heat the clusters while thermalizing their injection energy. At high injection energies the clusters can be heated to the point where they anneal (isomerize) or even fragment. Previous studies have shown that the polycyclic polyyne ring isomers for medium sized carbon clusters ($n \sim 40-70$) can anneal into roughtly spherical closed-cage fullerenes and that this structural conversion may be an important step in the gas-phase synthesis of fullerenes.[17-20]

Experimental Methods

The tandem quadrupole injected ion drift tube apparatus used for the studies reported here has been described in detail previously.[21,22] Carbon cluster ions are generated by pulsed laser vaporization of a carbon rod in a continuous flow of helium buffer gas. For some of the studies reported here a high-energy electron beam was injected into the buffer gas flow around 1 cm from where the clusters exit the source. This serves to increase the abundance of smaller cluster ions (by up to two orders of magnitude). After exiting the source, the cluster ions are focussed into a quadrupole mass spectrometer where a single cluster size is mass selected. The size-selected cluster ions are then focussed into a low-energy ion beam and injected into the drift tube at energies of 50–400 eV. In most experiments the drift tube contains helium buffer gas at a pressure of approximately 5 Torr. In a few experiments neon at around 2 Torr was employed (for reasons which will become apparent below). The drift field used in all experiments reported here was 13.12 V/cm, and the drift tube was 7.6 cm long. After traveling across the drift tube some of the ions exit through a small aperture and are focussed into a second quadrupole mass spectrometer. They are subsequently detected with an off-axis collision dynode and dual microchannel plates. The second mass spectrometer is used to examine the fragments that result when ions are injected into the drift tube at high injection energies.

The mobility of an ion is related to its drift velocity, v_D, through the expression

$$K = v_D/E \quad (1)$$

where E is the electric field across the drift tube.[23] The amount of time that it takes for the cluster ions to travel across the drift tube is measured by injecting 50-μs pulses of size-selected clusters and recording their arrival time distribution at the detector. The drift time distribution (DTD) is then obtained by subtracting, from the time scale, the time that the ions spend traveling from the exit aperture of the drift tube to the detector.

Results

Ion Mobility Measurements. Figure 1 shows representative drift time distributions for several carbon clusters in the 100–320 atom size range. These distributions were recorded with a helium buffer gas and with sufficiently low injection energies that no significant annealing or fragmentation occurs. Thus they represent the relative abundances of isomers generated in the laser vaporization source. All of the features in the drift time distributions shift to longer times with increasing cluster size because of the increase in the physical size of the cluster. The dominant feature in the drift time distributions is the relatively narrow peak at short drift times. This peak correlates with the feature attributed to the fullerene isomer for carbon clusters with $n < 70$, an assignment that is verified below. There are small features in the drift time distributions shown in Figure 1 at slightly shorter times than the large peak attributed to the fullerene. As we will see below, these peaks have mobilities close to those expected for doubly charged fullerene isomers.

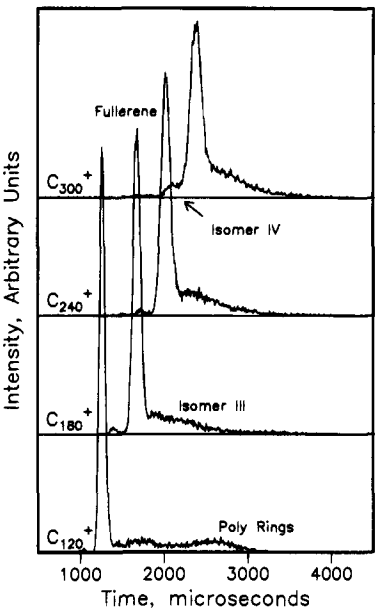

Figure 1. Drift time distributions recorded with helium buffer gas at low injection energy for C_n^+, n = 120, 180, 240, and 300. The time scale of each distribution has been scaled to a buffer gas number density corresponding to a drift tube pressure of 5.0 Torr and temperature of 298 K.

For the smallest cluster shown in Figure 1 (C_{120}^+), there is a broad feature at long times (around 2000–3000 μs) which appears to correlate with the polycyclic ring isomers observed for clusters with $n < 70$. The relative abundance of these isomers is rather small for the larger clusters studied here, diminishing further with increasing cluster size and vanishing altogether for clusters of more than approximately 160 atoms. For clusters with less than around 50 atoms, separate polycyclic ring isomers (attributed to monocyclic, bicyclic, tricyclic, and tetracyclic rings) have been resolved (for a given cluster size the drift time decreases slightly as the number of rings increases). The dominant ring isomer changes from monocyclic to bicyclic to tricyclic with increasing cluster size.[15] Conversely, for clusters with more than around 50 atoms, the individual ring isomers are no longer resolved, and instead they are represented by a broad feature, which presumably consists of a variety of different ring isomers. The variation in the average mobility of this feature with cluster size suggests that the average number of rings continues to increase as the cluster becomes larger. By the time the cluster reaches 120 atoms, the polycyclic rings are all more than tetracyclic.

Recently, Lagow et al. have suggested that a substantial fraction of the large carbon clusters generated by laser vaporization of graphite are long polyacetylene chains.[10] Linear chains have been identified in ion mobility studies of carbon cluster cations containing up to 10 atoms.[15] However, for slightly larger clusters, where the chains are flexible enough to form a ring,

(15) von Helden, G.; Hsu, M.-T.; Gotts, N.; Bowers, M. T. *J. Phys. Chem.* **1993**, *97*, 8182.
(16) Jarrold, M. F.; Constant, V. A. *Phys. Rev. Lett.* **1991**, *67*, 2994.
(17) Hunter, J. M.; Fye, J. L.; Jarrold, M. F. *Science* **1993**, *260*, 784.
(18) Hunter, J. M.; Fye, J. L.; Jarrold, M. F. *J. Chem. Phys.* **1993**, *99*, 1785.
(19) Hunter, J. M.; Fye, J. L.; Roskamp, E. J.; Jarrold, M. F. *J. Phys. Chem.* **1994**, *98*, 1810.
(20) von Helden, G.; Gotts, N. G.; Bowers, M. T. *Nature* **1993**, *363*, 60.
(21) Jarrold, M. F.; Bower, J. E.; Creegan, K. *J. Chem. Phys.* **1989**, *90*, 3615.
(22) Jarrold, M. F. *J. Phys. Chem.* **1995**, *99*, 11.
(23) Mason, E. A.; McDaniel, E. W. *Transport Properties of Ions in Gases*; Wiley: New York, 1988.

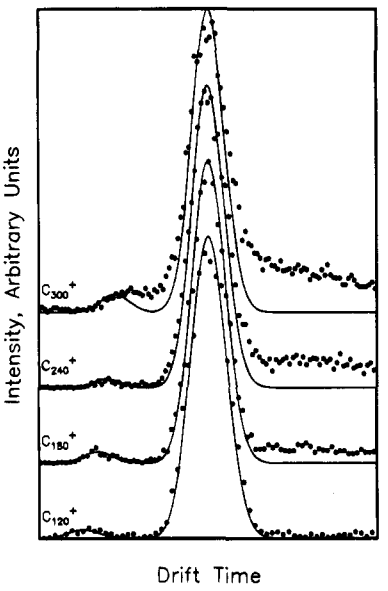

Figure 2. Comparison of the measured drift time distributions with those calculated by solution of the transport equation (eq 2) assuming that a single isomer is present. The points are the experimental measurements, and the line is the simulation. The axes have been scaled so that the fullerene peaks overlap.

the ring isomers dominate. There is no evidence for the presence of long polyacetylene chains in the cluster size range examined here.

While the polycyclic ring isomers vanish with increasing cluster size, another family of isomers emerges. This family of isomers is a broad feature extending from the fullerene toward the polycyclic ring isomers. The fact that these isomers appear as a broad distribution indicates the presence of a large number of slightly different isomers, analogous to the broad feature observed for the larger polycyclic ring isomers. We will refer to these isomers as isomer **III** (the rings and fullerenes can be viewed as the first two classes of isomers). Possible geometries for isomer **III** are discussed below.

The drift time distribution for a single isomer, obtained by solution of the transport equation for ions in the drift tube, is given by[23]

$$\Phi(t) = \int dt_p\, P(t_p) \frac{C(v_D + L/t)}{(Dt)^{1/2}} \left[1 - \exp\left(\frac{-r_0^2}{4Dt}\right)\right] \exp\left(\frac{-(L - v_D t)^2}{4Dt}\right) \quad (2)$$

In this expression r_0 is the radius of the entrance aperture, $P(t_p)$ dt_p is the distribution function of the pulse of ions entering the drift tube, C is a constant, and D is the diffusion constant, which under the low field conditions employed here is given by Kk_BT/e. Comparison of the measured drift time distributions to those calculated from eq 2 can be used to ascertain whether the observed feature results from several isomers with slightly different mobilities or appears to result from only a single isomer.[24] Such a comparison of the measured and calculated drift time distributions is shown in Figure 2 for C_{120}^+, C_{180}^+, C_{240}^+, and C_{300}^+. In order to facilitate direct comparison, the drift time distributions have been scaled so that the fullerene peaks overlap and are the same intensity. For C_{120}^+ and C_{180}^+ (as well as other clusters in this size range) the agreement is excellent, but deviations become increasingly apparent for the larger clusters. In addition to the large peaks in the middle of the time scale of Figure 2, we also show smaller peaks (at shorter times) calculated with the parameters expected for doubly charged fullerenes. It is clear that the small peaks at shorter times in the measured distributions have the drift times expected for doubly charged fullerenes. For the smaller clusters it is possible to confirm whether a peak is due to a doubly charged cluster by turning off the electron gun and examining the ions generated directly in the laser vaporization plasma. Because these ions spend longer in the source, the doubly charged ions are usually depleted by charge transfer processes and consequently are either not observed or are much less abundant. While for clusters with less than 200 atoms the small peak diminished or disappeared when the electron gun was turned off, for the larger carbon clusters ($n > 200$) the small peak remained (and in some cases increased) when the electron gun was turned off. This behavior may occur because the second ionization energy of the large fullerenes approaches the first; an alternative explanation is provided below.

It is clear from Figure 2 that there are substantial discrepancies between the measured and calculated distributions for C_{240}^+ and C_{300}^+. On the long-time side of the fullerene, this discrepancy can be largely attributed to the overlap of the fullerene with isomer **III**. The agreement between the measured and calculated distributions becomes worse with increasing cluster size as the relative abundance of isomer **III** increases. When the injection energy is increased and isomer **III** anneals away (see below), the agreement between the measured and calculated distributions improves dramatically. For C_{300}^+ (and other clusters in this size range) there is a significant disrepancy between the calculated and measured distributions at short times. It appears as though there is a significant amount of intensity between the fullerene peak and the expected location of the doubly charged fullerene. This component does not anneal away when the injection energy is increased, and so it may represent the emergence of a new family of isomers with larger mobilities than the fullerenes. We will refer to these isomers as isomer **IV**.

The mobilities of the fullerenes were determined by fitting the measured DTD with distributions calculated using eq 2, treating the drift velocity as an adjustable parameter. Because of the relatively long drift times of the large fullerenes studied here and the problem of the overlap with isomer **III** and isomer **IV**, this approach provides a slightly more accurate value for the mobility than can be obtained by simply inserting the average drift velocity into eq 1. By convention, the measured mobility is converted into a reduced mobility using[23]

$$K_0 = K \frac{P}{760} \frac{273.2}{T} \quad (3)$$

To facilitate comparison with mobilities estimated for particular fullerene geometries, the reduced mobilities were then divided into the mobility of a sphere with a surface area equal to that estimated for the fullerene. The surface area was estimated using the dimensions of the pentagons in C_{60} and a model that interpolates the dimensions of the hexagons between that found in C_{60} and bulk graphite. The mobilities of the spheres were then determined from[23]

$$K_0 = \frac{(18\pi)^{1/2}}{16}\left[\frac{1}{m_I} + \frac{1}{m_B}\right]^{1/2} \frac{e}{(k_BT)^{1/2}} \frac{1}{Q_{sph}} \frac{1}{N} \quad (4)$$

where m_I and m_B are the masses of the ion and buffer gas, respectively, N is the buffer gas number density, and Q_{sph}, the hard sphere collision cross section for the sphere, is given by

$$Q_{sph} = \pi(r_{sph} + r_{sph\text{-}He})^2 \quad (5)$$

In this expression r_{sph} is the radius of the sphere and $r_{sph\text{-}He}$ is

(24) Jarrold, M. F.; Bower, J. E. *J. Chem. Phys.* **1993**, *98*, 2399.

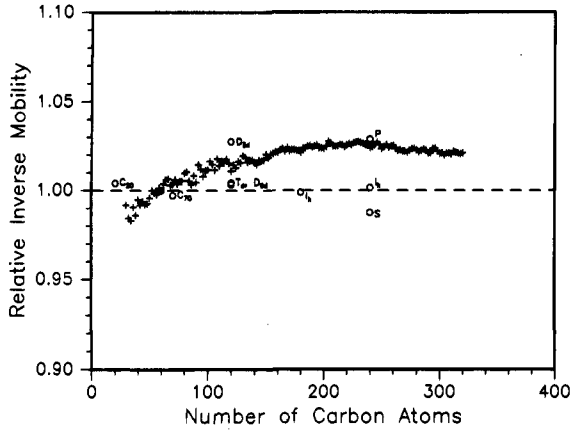

Figure 3. Relative inverse mobilities of the fullerene isomers as a function of the number of carbon atoms (+). Variations in the mobilities due to changes in the physical size of the fullerenes have been removed by dividing the experimental inverse mobilities by the calculated inverse mobilities of a sphere with a surface area approximately equal to that of a spheroidal fullerene (see text). Relative mobilities calculated from atomic coordinates of minimum energy geometries are also plotted (O) for C_{20}, C_{60}, C_{70}, C_{120} (T_d, D_{6d}, and D_{5d}), C_{180} (I_h), and C_{240} (I_h, S, and P) (see text).

the hard sphere collision distance for collisions of the spherical carbon cluster with helium. $r_{sph\text{-}He}$ was adjusted so that the calculated mobility for C_{60}^+ is equal to the measured value, and thus the relative inverse mobility of C_{60} (the measured mobility divided into that estimated using the sphere model) equals one. A relative inverse mobility of greater than one indicates that the effective size of the fullerene is larger than that predicted by the sphere model. The relative inverse mobilities of the fullerene isomers are plotted in Figure 3. The experimental data are an average of at least two independent measurements which generally differ by less than 1%. The results in Figure 3 show that the relative inverse mobilities systematically diverge from the predictions of the spherical model. The relative inverse mobilities of the smaller fullerenes ($n < 60$) are slightly lower than predicted by the spherical model while those for the larger fullerenes ($n > 60$) are slightly larger.

Annealing and Dissociation Studies. As the cluster ions enter the drift tube their injection energy is thermalized by collisions with the buffer gas. During this process the clusters are rapidly heated and then cooled by further collisions with the buffer gas. If the injection energy is increased, then the clusters may be heated to the point where they anneal or dissociate. The following discussion focuses on the results of annealing and dissociation studies for C_{120}^+, C_{180}^+, C_{240}^+, and C_{300}^+.

At a low injection energy (100 eV) the DTD for C_{120}^+ (shown in Figure 1) exhibits a sharp peak corresponding to the fullerene and two broad distributions at longer times. As noted above, the broad distribution at 2000−3000 μs for C_{120}^+ appears to correlate with the feature that has been attributed to polycyclic polyyne ring isomers for clusters with less than 70 atoms. Previous studies of carbon clusters with up to 70 atoms have shown that when the injection energy is raised, some of the polycyclic polyyne rings anneal into fullerenes. A minimum of around 40 atoms is required for fullerene formation from the rings, and the efficiency of fullerene formation increases slowly with cluster size to reach around 80% at C_{60}^+.[19] The low abundance of the polycyclic ring isomers for the larger clusters such as C_{120}^+ must presumably reflect the conversion of these isomers into fullerenes as they grow in the source, so that most of them do not survive to reach C_{120}^+.

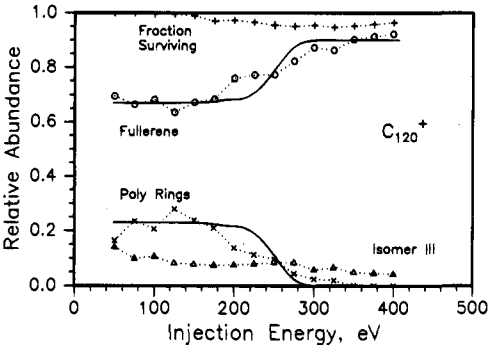

Figure 4. Relative abundance of the C_{120}^+ isomers as a function of injection energy into 5 Torr of helium. The line is a simulation of the injection energy threshold for conversion of the polycyclic rings into fullerenes (see text).

From what is known about the smaller polycyclic ring isomers, we expect that for the larger clusters these isomers will readily anneal into fullerenes. In Figure 4 we show the relative abundances of the various C_{120}^+ isomers plotted against injection energy. As expected the polycyclic ring isomers disappear as the injection energy is raised, while the relative abundance of the fullerene increases. Some fragmentation also appears to be associated with this process, with around 20% of the polycyclic rings dissociating to give products such as C_{118}^+, C_{116}^+, and C_{114}^+. Mobility measurements show that these fragments are fullerenes. Conversion of the rings into fullerenes is a very exothermic process, and these fragments probably result from the dissociation of the hot fullerene generated by annealing of the polycyclic rings. Similar fragmentation processes have been observed for the smaller clusters. Considerably less fragmentation is apparently observed for the larger clusters studied here, although discrimination effects may influence these relative abundances.

An estimate of the activation energy for this annealing process can be obtained from the injection energy threshold using a simple modified impulsive collision model to estimate the fraction of the injection energy converted into internal energy and RRKM (Rice, Ramsperger, Kassel, and Marcus) theory[25] to account for the statistical nature of the annealing process.[26] The solid lines in Figure 4 show the results of such simulations, and the estimated activation energy determined from these simulations is 1.8 eV. This can be compared with the estimated activation energies for C_{40}^+ and C_{70}^+ of 2.8[18] and 2.4 eV,[19] respectively. These activation energies should be treated as estimates because it is not possible to rigorously determine the degree of collisional excitation that occurs as the clusters enter the drift tube, and there is some uncertainty in the statistical treatment of the annealing process. Formation of fullerenes from the rings is believed to involve generation of a fullerene precursor, consisting of a partial network of pentagons and hexagons, followed by closure of the fullerene cage.[19,27] The activation energy for fullerene formation decreases significantly with increasing cluster size presumably because the strain energy that builds up during formation of the fullerene precursor, or during the first steps along the road to fullerene formation, decreases for the larger clusters.

As can be seen from Figure 4, C_{120}^+ isomer **III** (isomers with mobilities between those of the fullerene and the polycyclic

(25) Robinson, P. J.; Holbrook, K. A. *Unimolecular Reactions*; Wiley: London, 1972. Forst, W. *Theory of Unimolecular Reactions*; Academic: New York, 1973.

(26) Jarrold, M. F.; Honea, E. C. *J. Phys. Chem.* **1991**, *95*, 9181.

(27) Schweigert, V. A.; Alexandrov, A. L.; Morokov, Y. N.; Bedanov, V. M. *Chem. Phys. Lett.* **1995**, *235*, 221.

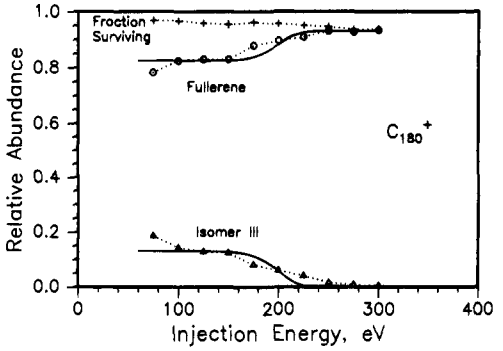

Figure 5. Relative abundance of the C_{180}^+ isomers as a function of injection energy into 2 Torr of neon. The line is a simulation of the injection energy threshold for disappearance of the non-fullerene isomers (see text).

rings) does not all anneal or fragment with injection energies up to 400 eV. The amount of energy deposited into the clusters as they enter the drift tube can be increased by employing a heavier buffer gas such as neon instead of helium. With neon, isomer **III** disappears at injection energies of around 200 eV, from which the activation energy is estimated to be around 2.5 eV. It seems likely that isomer **III** anneals into the fullerene geometry because we do not see a significant increase in the amount of fragmentation. However, the relative abundance of isomer **III** is rather small for C_{120}^+, so it is possible that these isomers could fragment into a broad range of different products, and the relative abundance of each of these products could be too small for us to detect.

For C_{180}^+ the polycyclic ring isomers are no longer present in the isomer distribution coming from the source. Surprisingly, a small amount of fragmentation is observed for this cluster even with low injection energies into helium buffer gas. The products result mainly from the loss of C_{18}, with smaller amounts resulting from the loss of C_{20}, C_{22}, and other even-numbered fragments. In fact, this low-energy fragmentation process is observed for all of the larger carbon clusters. It seems feasible that this process results from the fragmentation of a loosely bound complex such as a ring weakly attached to the surface of a fullerene. Note that a C_{18} ring, with $4n + 2$ atoms, possesses aromatic stabilization, and this probably accounts for why it is a favored product.

For C_{180}^+ with a helium buffer gas, the relative abundances of the fullerene and isomer **III** remain essentially unchanged as the injection energy is increased to 400 eV. Figure 5 shows a plot of the results recorded with neon buffer gas. This figure shows the relative abundances of the fullerene and isomer **III** plotted against injection energy. These experiments were performed with a buffer gas pressure of around 2 Torr. This lower pressure was employed because at a pressure of 5 Torr there was evidence for discrimination against isomers with long drift times, at the lower injection energies. As can be seen from the figure, isomer **III** disappears at injection energies around 150−250 eV. Analysis of the injection energy threshold yields an estimated activation energy of around 2.3 eV. Again, as we see no significant increase in the amount of fragmentation, it seems likely that isomer **III** anneals into the fullerene.

The behavior of C_{240}^+ is similar to that described above for C_{180}^+. Around 3% of the C_{240}^+ ions dissociate when injected into helium at 50 eV. The products result mainly from loss of C_{18}, and drift time distributions recorded for the C_{222}^+ product ion show that its mobility is the same as the C_{222}^+ fullerene isomer coming directly from the source. The relative abundance of C_{240}^+ isomer **III** remains essentially unchanged as the injection energy is raised to 400 eV with a helium buffer gas. With a neon buffer gas, isomer **III** disappears with injection energies around 225−325 eV. No significant increase in the amount of fragmentation is observed so isomer **III** presumably anneals into the fullerene. Analysis of the injection energy threshold leads to an estimated activation energy of around 2.3 eV.

The behavior of C_{300}^+ is similar to that described above for C_{180}^+ and C_{240}^+. Most of isomer **III** anneals away at high injection energies in neon buffer gas. On the other hand, isomer **IV** (the isomers with shorter drift times than the fullerene) does not anneal away, even with an injection energy of 400 eV into neon. This indicates that isomer **IV** is relatively stable. A plausible geometry for these isomers will be discussed below.

Discussion

The Nature of Isomer III and Isomer IV. A definitive structural assignment for isomer **III**, the isomers with drift times between the fullerenes and polycyclic rings, is difficult because of the absence of distinct peaks in the drift time distributions. However, it is possible to piece together information from the mobility measurements and the annealing and dissociation studies to provide a plausible structural assignment for these isomers.

For the smaller carbon clusters there are two main families of isomers: the fullerenes and the polyyne rings. There is, however, another type of isomer present. It is represented by a relatively narrow peak with a drift time between that of the rings and the fullerene. This isomer has recently been assigned to roughly planar graphitic fragments.[28] It never amounts to more than a few percent of the total isomer distribution for clusters with 30−70 atoms. However, because the mobility of this isomer is between that of the fullerene and the rings, it is clearly a plausible candidate for isomer **III**. Graphite is the most stable phase of bulk carbon, and while the dangling bonds at the edges of graphite fragments destabilize them, the destabilization decreases with increasing cluster size because the fraction of carbon atoms on the edges decreases. Thus the estimated heat of formation for planar graphite fragments decreases from around 0.8 eV/atom for C_{60} to approximately 0.44 eV/atom for C_{300}.[28]

To determine how the mobilities of graphitic fragments compare with the mobilities of isomer **III**, mobilities were estimated for some model graphitic fragment geometries. The mobilities were estimated using eq 3 with the collision cross section obtained by averaging over all orientations of the model geometry in space:[29]

$$Q = \int_0^{\pi} d\theta \cos\theta \int_0^{\pi} d\phi \, q(\theta,\phi) \qquad (6)$$

where $q(\theta,\phi)$ is the calculated collision cross section for an orientation defined by angles θ and ϕ. The hard-sphere collision distance in these calculations was taken to be 2.8 Å (which was obtained by fitting the measured mobility of C_{60}^+). Figure 6 shows the drift time distribution recorded for C_{240}^+ with a helium buffer gas, with lines showing the estimated drift times for a variety of different geometries. The estimated drift time of the planar, roughly circular graphite sheet is 2600 μs, which is longer than the drift times of most of the isomer **III** distribution. Planar graphitic fragments with longer drift times can be obtained by distortion from the roughly circular shape. There are two ways to obtain graphite fragments with shorter drift times: either distort from a planar geometry, or stack

(28) Shelimov, K. B.; Hunter, J. M.; Jarrold, M. F. *Int. J. Mass Spectrom. Ion Proc.* **1994**, *138*, 17.
(29) Jarrold, M. F.; Bower, J. E. *J. Chem. Phys.* **1993**, *98*, 2399.

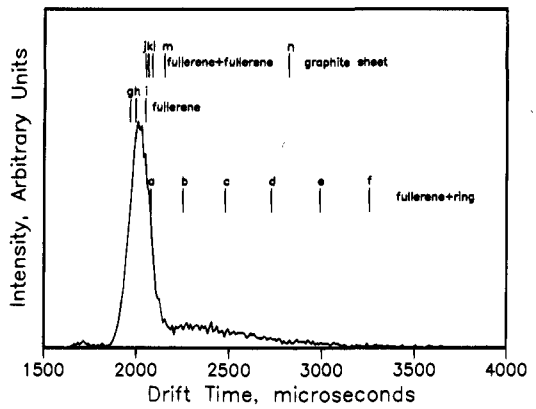

Figure 6. Drift time distribution for C_{240}^+ recorded with a helium buffer gas at an injection energy of 250 eV. The lines show estimated drift times of several structures. The letters correspond to the following geometries: (a) C_{230} fullerene + C_{10} ring; (b) C_{220} fullerene + C_{20} ring; (c) C_{210} fullerene + C_{30} ring; (d) C_{200} fullerene + C_{40} ring; (e) C_{190} fullerene + C_{50} ring; (f) C_{180} fullerene + C_{60} ring; (g) spheroid and MNDO icosahedral fullerene; (h) LDA *S*; (i) LDA *P*; (j) C_{120} fullerene + C_{120} fullerene; (k) C_{180} fullerene + C_{60} fullerene; (l) C_{120} fullerene + 2 C_{60} fullerenes (orthogonal); (m) C_{120} fullerene + 2 C_{60} fullerenes (linear); (n) spiral graphite sheet.

several smaller graphitic fragments together. A nonplanar geometry is readily obtained for a graphite fragment by replacing hexagons by pentagons. The van der Waals interaction for a stack of two graphitic fragments, each containing 120 atoms, is estimated to amount to around 4.8 eV,[30] so these geometries should be stable enough to survive injection into the drift tube.

Another plausible structure for isomer **III** is carbon fragments, such as rings, covalently bound to the outside of fullerenes. Precedence for these types of geometries is found in the condensed phase, where fullerene derivatization via [2 + 2] or [4 + 2] Diels–Alder cycloaddition reactions with C_{60} and C_{70} can occur with high yields.[31] In gas-phase selected-ion flow tube experiments, there is evidence for [4 + 2] cycloaddition of 1,3-cyclopentadiene and 1,3-cyclohexadiene to C_{60}^+ and C_{70}^+.[32] Because the polyyne rings are known to be abundant isomers for carbon clusters with less than 40 carbon atoms, it is not unreasonable to suggest that they may undergo cycloaddition reactions with the fullerenes. As a model for geometries with a ring attached to the outside of a fullerene, we employed a sphere to represent the fullerene and a toroid[33] to represent the ring. The distance between the fullerene and the ring was set to 1.6 Å in these calculations, which is the distance determined by Strout et al. for the [2 + 2] addition product of two C_{60} molecules.[34] The estimated mobilities for the fullerene + ring geometry are shown in Figure 6 for C_n (fullerene) + C_m (ring) with $n + m = 220 + 20$, $210 + 30$, $200 + 40$, $190 + 50$, and $180 + 60$. While we assume that the ring is a monocyclic ring, bicyclic and tricyclic rings attached to fullerenes will not have substantially different mobilities. It is also possible that isomers consisting of two separate rings attached to a fullerene could be present. However, since the relative abundance of isomer **III** is less than that of the fullerene, it is likely that the relative abundance of isomers with two rings attached to a fullerene will be low. It is apparent from the results shown in Figure 6 that the fullerene + ring model can readily account for the broad distribution of non-fullerene isomers. Indeed, the distribution of non-fullerene isomers appears to correspond to the relative abundance of the ring isomers for the smaller clusters.

From the above discussion it appears that both the graphitic fragments (including the nonplanar and/or stacked graphite sheets) and the fullerene + ring geometry have mobilities which can account for isomer **III**. There are, however, several reasons to believe that the fullerene + ring geometry is more plausible. First, quantum chemical calculations for small graphitic fragments indicate that the nonplanar geometry is less stable than the planar geometry,[35] and only planar roughly-circular graphitic fragments are observed for the smaller clusters ($n = 30-70$).[28] Second, formation of a stack of graphite sheets requires individual sheets as precursors, yet the relative abundance of the planar roughly-circular graphite sheets for the smaller clusters is always less than a few percent.[28] Third, the estimated activation energies for annealing of the non-fullerene isomers are relatively low, and considerably smaller than the activation energies expected for the rearrangement of carbon networks (the activation energy for the Stone–Wales isomerization has been estimated to be around 5 eV[36]). Furthermore, the observed activation energies are essentially the same as those observed for annealing of the ring isomers into fullerenes for the smaller clusters.

For the largest clusters studied another family of isomers with shorter drift times than the fullerene begins to emerge. Isomer **IV** does not anneal or dissociate even with injection energies of 400 eV into neon, which indicates that it is relatively stable. Probably the most plausible geometry for these isomers is a fullerene cage encapsulating a carbon fragment. If this carbon fragment is a fullerene, then this isomer would be a nested fullerene or a bucky-onion. A two-shell nested fullerene consisting of a C_{60} surrounded by a C_{240} would have the same drift time as C_{240}^+, and approximately the same drift time as C_{600}^{2+} fullerene. This suggests an alternative explanation for the small peaks at short times in the drift time distributions of the larger clusters: that they are due to nested fullerenes rather than doubly charged fullerenes. This would explain why these features persist when the electron gun is turned off, while the doubly charged fullerenes for the smaller clusters disappear. Even if the cluster ions with mobilities close to that expected for the doubly charged fullerene are indeed doubly charged, the remaining isomers with drift times between the doubly charged C_{600}^{2+} and singly charged C_{300}^+ fullerene may result from nested fullerenes with less than 60 carbon atoms inside—around 30–40 endohedral carbon atoms is consistent with the experimental data. Note that in order for this many carbon atoms to fit inside a fullerene with 260–270 carbon atoms, they must also have a fullerene geometry. So for these nested fullerenes the inner fullerene must be somewhat smaller than the cavity provided by the outer shell. Theoretical estimates indicate that the nested fullerene geometry should be less stable than the single cage fullerene for clusters in this size regime.[8,9] However, nested fullerenes as small as around $C_{50}@C_{230}$ (C_{50} inside a C_{230}) have been observed in electron microscope studies.[37] The observation of an inner fullerene with less than 60 atoms has been attributed to the stabilizing effect of the onion-like structure.

(30) This estimate of the van der Waals interaction between two roughly circular C_{120} graphite sheets employed the van der Waals parameters in: Rafizadeh, H. A. *Physica* **1974**, *74*, 135.

(31) Zhang, X.; Romero, A.; Foote, C. *J. Am. Chem. Soc.* **1993**, *115*, 11024.

(32) Becker, H.; Javahery, G.; Petrie, S.; Bohme, D. K. *J. Phys. Chem.* **1994**, *98*, 5591.

(33) Hunter, J. M.; Fye, J. L.; Jarrold, M. F. *J. Phys. Chem.* **1993**, *97*, 3460.

(34) Strout, D. L.; Murry, R. L.; Xu, C.; Eckhoff, W. C.; Odom, G. K.; Scuseria, G. E. *Chem. Phys. Lett.* **1993**, *214*, 576.

(35) Raghavachari, K.; Zhang, B.; Pople, J. A.; Johnson, B. G.; McGill, P. M. W. *Chem. Phys. Lett.* **1994**, *220*, 385.

(36) Yi, J.-Y.; Bernholc, J. *J. Chem. Phys.* **1992**, *96*, 8634.

(37) Ugarte, D. *Europhys. Lett.* **1993**, *22*, 45.

The Shapes of the Fullerene Isomers. There have been numerous theoretical studies of closed-cage fullerene structures for carbon clusters containing up to several hundred atoms. Although *ab initio* quantum chemical calculations are prohibited by the large number of atoms in these systems, approximate methods such as density functional theory and MNDO have been utilized to predict ground-state structure and relative stability.[38,39] In general, the results of these calculations suggest that the more highly symmetric geometries are the more stable. Relative inverse mobilities have been estimated for calculated geometries of fullerenes containing 20,[40] 60,[41] 70,[41] 120,[42] 180,[43] and 240[43,44] carbon atoms. All geometries were obtained from calculations performed at the MNDO level, except for the *S* (roughly spherical) and *P* (polyhedrally faceted) isomers of C_{240}, which were obtained from calculations performed using the density functional method.[44] Mobilities were estimated for these geometries using the approach outlined above for the graphite sheets. The estimated relative inverse mobilities for the calculated geometries are shown plotted in Figure 3. As can be seen from the figure, the mobilities of the calculated geometries all lie close to the measured mobilities, which confirms that these isomers are fullerenes. Comparison of the measured and calculated mobilities suggests that the larger fullerenes may be slightly distorted from a spherical geometry. For example, the calculated mobility for the polyhedrally faceted (P) C_{240} isomer appears to be in excellent agreement with the measured mobility for this clusters. This observation appears to conflict with the theoretical calculations which suggest that the spherical (S) isomer is the more stable.[44] However, in our estimates of the mobilities of the calculated structures we employed a hard sphere model to determine the collision cross section. Recently we have employed a more sopisticated approach and determined mobilities from trajectory calculations using a realistic intermolecular potential between the fullerene and the buffer gas.[45] These calculations show that while the hard sphere approximation is reasonably good, the long range potential can cause significant deviations. The results of these calculations will be discussed in more detail elsewhere.

The number of possible fullerene isomers containing isolated pentagons increases rapidly as the number of atoms increases.[46] While many of these isomers have very similar average collision cross sections, such that it is not possible to separate them with the time resolution available in our drift tube experiment, the mobility estimates described above show that fullerenes with slightly different shapes will have different mobilities. Drift time distributions calculated using eq 2 are in good agreement with the measured drift time distributions (after the non-fullerene isomers are annealed), suggesting that only a single fullerene isomer or several fullerene isomers with similar shapes are present. Also, note that the mobilities of the fullerenes change smoothly with cluster size (see Figure 3); this indicates that there are no abrupt changes in the shapes of the fullerenes with size.

The Mechanism of Giant Fullerene Formation. It now seems clear that small fullerenes are formed by isomerization of polycyclic rings, and the rings are formed by coalescence of smaller rings. However, these fullerene precursors disappear for clusters with around 160 atoms, so obviously the larger fullerenes must be synthesized by some other mechanism. Laser ablation of fullerene films has been shown to result in the coalescence of fullerenes to form larger carbon clusters (such as C_{118}^+ and C_{120}^+ from C_{60} films).[47] Because these coalescence products are unusually stable toward dissociation it has been suggested that they are single-cage fullerene structures. Thus fullerene coalescence could be a plausible mechanism for generating the larger fullerenes. Ion mobility measurements of C_{120}^+ ions generated from fullerene films showed that dimer-like geometries are also produced in addition to the single-cage fullerene geometry.[48] Some of the dimer-like geometries readily fragment to give C_{60}^+ and C_{60}. Mobility estimates suggest that "dimers" will not be resolved from the fullerenes for clusters with more than 180 atoms. That is, $(C_{90})_2^+$ dimer and C_{180}^+ fullerene have very similar mobilities. For clusters containing more than 180 atoms, therefore, fused fullerene structures could in fact be present at low injection energies and anneal into a fullerene as the injection energy is raised, but this coalescence process would not be detectable in the drift time distribution. An indication that this type of coalescence process is occurring would be dissociation of the dimer by loss of large carbon fragments. No such fragmentation processes were observed. However, if the dissociation products were distributed over a large number of ions, their intensities may be too small for us to detect.

The results presented above suggest that coalescence of fullerenes and rings followed by isomerization into a closed shell fullerene is the most likely mechanism of giant fullerene formation. This mechanism is favored for several reasons. First, the observation of [2 + 2] and [4 + 2] addition reactions of fullerenes indicates that coalescence of rings and fullerenes should be a facile process. Second, the ring isomers are the dominant isomers present for the smaller carbon clusters so coalescence of the rings and fullerenes should occur with a fairly high probability. Third, the estimated activation energies for annealing of the non-fullerene isomers of these large carbon clusters are similar to the activation energies estimated for isomerization of the rings into fullerenes for smaller clusters. Finally, the rings are substantially less stable than the fullerenes, so that the energy released when they start to anneal is available to drive the formation of a spheroidal fullerene. Note that the energy released during this isomerization process is dissipated over a larger number of degrees of freedom, and it is insufficient to fragment the nascent fullerene (unlike conversion of rings to fullerenes for the smaller clusters).

Conclusions

Ion mobility measurements have been used to probe carbon cluster ions with 100−320 atoms. The dominant isomer present is the single-shell fullerene. The polycyclic ring isomers, which are the dominant isomers present for small clusters, vanish for clusters with around 160 atoms. There is no evidence for the presence of long polyacetylene chains. A new family of isomers (isomer **III**) emerges at around 100 atoms and becomes more abundant with increasing cluster size. These new isomers are probably carbon rings covalently bound to the outside of fullerenes. At high injection energies it appears that they can be annealed into fullerenes. For clusters with around 270 atoms

(38) Murry, R. L.; Scuseria, G. E. *J. Phys. Chem.* **1994**, *98*, 4212.
(39) Zhang, B. L.; Wang, C. Z.; Ho, K. M.; Chan, C. T. *J. Chem. Phys.* **1993**, *98*, 3095.
(40) Shelimov, K. B. Private communication.
(41) Raghavachari, K. Private communication.
(42) Murry, R. L.; Colt, J. R.; Scuseria, G. E. *J. Phys. Chem.* **1993**, *97*, 4954.
(43) Bakowies, D.; Thiel, W. *J. Am. Chem. Soc.* **1991**, *113*, 3704.
(44) York, D.; Lu, J. P.; Yang, W. *Phys. Rev. B* **1994**, *49*, 8526.
(45) Jarrold, M. F.; Hunter, J. M. To be submitted for publication.
(46) Manolopoulos, D. E.; Fowler, P. W. *J. Chem. Phys.* **1992**, *96*, 7603.
(47) Yeretzian, C.; Hansen, K.; Diederich, F.; Whetten, R. L. *Nature* **1992**, *359*, 44.
(48) Hunter, J. M.; Fye, J. L.; Boivin, N. M.; Jarrold, M. F. *J. Phys. Chem.* **1994**, *98*, 7440.

another family of isomers (isomer **IV**) begins to emerge at shorter drift times than the single-cage fullerene. These isomers do not anneal or fragment at high injection energies. They may be nested fullerenes.

The polycyclic ring isomers which are the precursors for the smaller fullerenes vanish around 160 atoms, so giant fullerene formation must occur through other precursors via a different mechanism. The results presented here suggest that giant fullerene formation involves coalescence of fullerenes and rings, followed by annealing into a giant fullerene.

Acknowledgment. We gratefully acknowledge the support of this work by the National Science Foundation (Grant No. CHE-9306900) and the Petroleum Research Fund, administered by the American Chemical Society. We thank Dr. David Clemmer for assistance with the modeling. We are also grateful to several groups for providing atomic coordinates of fullerene isomers: Prof. G. Scuseria for C_{120}, Prof. W. Yang and his collaborators for two isomers of C_{240}, Prof. W. Thiel for C_{240} and C_{180}, and Dr. K. Raghavachari for C_{60} and C_{70}.

JA9516468